

Fundamental limitations on photoisomerization from thermodynamic resource theories

Nicole Yunger Halpern^{1,2,3,4} and David T. Limmer^{5,6,7}

¹*Institute for Quantum Information and Matter,*

California Institute of Technology, Pasadena, CA 91125, USA

²*Kavli Institute for Theoretical Physics, University of California, Santa Barbara, CA 93106, USA*

³*ITAMP, Harvard-Smithsonian Center for Astrophysics, Cambridge, MA 02138, USA*

⁴*Department of Physics, Harvard University, Cambridge, MA 02138, USA*

⁵*Department of Chemistry, University of California, Berkeley, CA 94720, USA*

⁶*Kavli Energy NanoSciences Institute, University of California, Berkeley, CA 94720, USA*

⁷*Lawrence Berkeley National Laboratory, University of California, Berkeley, CA 94720, USA*

(Dated: May 30, 2022)

Small, out-of-equilibrium, and quantum systems defy simple thermodynamic expressions. Such systems are exemplified by molecular switches, which exchange heat with a bath and which can photoisomerize, or change conformation upon absorbing light. The likelihood of photoisomerization depends on kinetic details that couple the molecule’s internal energetics with its interaction with the bath, hindering predictions. We derive simple, general bounds on the photoisomerization yield, using a resource-theory model for thermodynamics. The resource-theory framework is a set of mathematical tools, developed in quantum information theory, for modeling any setting in which constraints restrict the operations performable and the systems accessible. Resource theories are being used to generalize thermodynamics to small and quantum settings. Specifically, we use the thermomajorization preorder, a resource-theory generalization of the second law. Thermomajorization follows from the minimal assumptions of energy conservation and a fixed bath temperature. Using thermomajorization, we upper-bound the photoisomerization yield. Then, we compare the bound with expectations from detailed balance and from simple Lindbladian evolution. Our minimal assumptions constrain the yield tightly if a laser barely excites the molecule, such that thermal fluctuations drive conformation changes, and weakly if the laser excites the molecule to one high-energy eigenstate. We also quantify and bound the coherence in the molecule’s post-photoisomerization electronic state. Electronic coherence cannot boost the yield in the absence of extra resources, we argue, because modes of coherence transform independently via resource-theory operations. This work illustrates how thermodynamic resource theories can offer insights into complex quantum processes in nature, experiments, and synthetics.

Thermodynamics quantifies ideal processes with simple expressions and constrains processes that deviate from the ideal. This simplicity vanishes in the face of small systems and intermediate time scales. Such realistic settings yoke work, heat, and entropy production to kinematic details, exposing each as a fluctuating quantity. Yet one can hope to bound kinematic results with general thermodynamic-style expressions. Examples have enjoyed theoretical and experimental success. For example, the fluctuation theorems and Jarzynski’s equality [1–3] constrain ensembles of irreversible transformations. These results govern experiments, including with single molecules [4, 5] and information engines [6–8]. Additionally, thermodynamic uncertainty relations [9, 10] have constrained the precision with which microscopic currents can be generated. These findings have relevance to molecular motors [11, 12] and self-assembly [13, 14]. Here, we derive bounds for the photoisomerization of molecular switches, leveraging the quantum-information (QI) tool of thermodynamic resource theories.

Small molecules photoisomerize in many natural and synthetic systems [15–20]. Example photoisomers include retinal in rhodopsin, a pigment in the retina [21], and green fluorescent protein, a chromophore used throughout molecular imaging [22]. Two conveniences

account for these molecular switches’ popularity. First, ultrafast femtosecond lasers offer control over photoisomerization [23–27]. Second, photoisomers can be synthesized easily, and one can easily encourage the expression of genes that code for isomers. Applications are widespread and include azobenzene-based solar-to-thermal fuels [28, 29] and functional polymers [25, 30]. Despite their usefulness and prevalence, photoisomers evade a complete understanding. Reasons include how experimental tools, such as time-resolved spectroscopy [31–34], allow one to follow only a subset of relevant degrees of freedom (DOFs). Additionally, computational tools for simulating these processes remain under active development [35–43].

Photoisomerization begins with a molecule in its thermal state, which is well-approximated by the lowest electronic energy eigenstate. The electronic energy levels depend on the heavy atoms’ coordinates, which are parameterized with an angle φ . The dependence follows from the electronic energy-level spacing’s far exceeding the energy spacings associated with the molecule’s vibrations and rotations [44]. The ground electronic level exhibits two wells, centered near $\varphi = 0$ and $\varphi = \pi$, separated by an energy barrier. These angles define two conformations, or isomers, of the molecule. Called *cis* and *trans* states, the isomers are shown schematically in Fig. 1. Low-lying

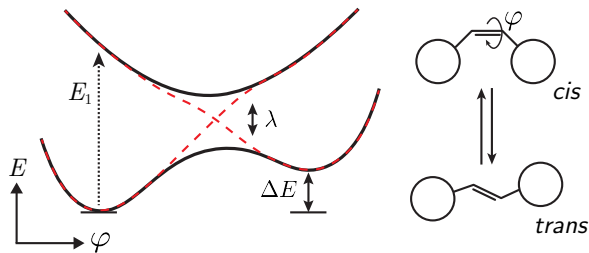


FIG. 1: Two representative potential-energy surfaces for the ground and excited electronic states of an isomer, as well as the *cis* and *trans* configurations associated with the ground-state minima. The black curves represent adiabatic states, or instantaneous energy eigenstates. The red curves represent diabatic states, which approximately equal adiabatic states at $\varphi = 0, \pi$.

excited electronic states can lack energy barriers. If excited by light, therefore, the molecule has the opportunity to change configurations while relaxing, in contact with its environment, back to the lower electronic level. The probability of changing conformation during relaxation is called the “photoisomerization yield.”

The yield is difficult to predict for several reasons. First, dynamical factors determine the yield over intermediate time scales. These times exceed the time needed for the electronic DOF to relax to its ground state but are shorter than the time over which the whole molecule thermalizes. This intermediacy precludes straightforward thermodynamic statements. Second, the postexcitation evolution involves nonadiabaticity [45], dissipation [45], and rare bath fluctuations [46]. Hence studying the evolution computationally is difficult, and few general guiding principles exist. We need a toolkit for deriving thermodynamic-style bounds on photoisomerization. These bounds should incorporate the coupling of quantum mechanical DOFs with small scales and thermal fluctuations. To construct such bounds, we use a resource theory.

Resource theories are simple models developed in QI theory [47, 48]. They are relevant when restrictions constrain the processes that can occur, called “free operations,” and the systems accessible, called “free systems.” Consider, as an example, a thermodynamic setting in which systems exchange heat with a bath at a fixed temperature. The first law of thermodynamics constrains processes to conserve energy, and only thermal states can be accessed easily. The corresponding resource theory’s free operations are called “thermal operations.” All non-free systems, e.g., systems not in states thermal with respect to the environment’s temperature, are “resources.” Resources have value because they can fuel tasks such as work extraction. Resource theories originated to quantify entanglement and to clarify which QI-processing tasks entanglement could facilitate [49]. Since then, resource theories have been developed for other valuable quantities, including reference frames [50–55], randomness used

in cryptography [47], coherence [56–58], “magic states” used in quantum computation [59], and thermodynamics [60–68].

Using a resource theory, one studies which systems R can transform into systems S under free operations ($R \mapsto S$); which cannot ($R \not\mapsto S$); how much of a resource W , such as work, is required to facilitate an otherwise impossible transformation ($R + W \mapsto S$ despite $R \not\mapsto S$); how many copies of S can be extracted from m copies of R ; and what, generally, is possible and impossible. Results govern arbitrarily small systems and coherent quantum states. In thermodynamic resource theories, averaging in a large-system limit reproduces results consistent with expectations from statistical mechanics. Hence resource theories offer the potential for formulating sharp, general statements about complex, quantum systems. We harness this potential for molecules undergoing photoisomerization.

The paper is organized as follows. First, we review the resource theory that models heat exchanges. We then model the molecule within the resource theory (Sec. I). We bound the isomerization yield by applying the resource theory’s thermomajorization preorder (Sec. II). The yield is tightly constrained, we find, if the light source barely excites the molecule, such that mainly thermal fluctuations drive conformational changes. If the light source fully excites the molecule to one high-energy eigenstate, thermomajorization constrains the yield weakly. In this case, kinetic fine-tuning can result in a perfect, unit photoisomerization yield.

We next quantify the energy coherence gained by the molecule during photoisomerization (Sec. III). We quantify the coherence with resource-theory monotones, functions that decrease monotonically under free operations and that quantify a system’s value. Specifically, we characterize the postisomerization state’s coherence with the Fisher information relative to the Hamiltonian. This coherence emerges after a dissipative Landau-Zener evolution, which we model within the resource theory. Electronic coherence, we argue further, cannot increase the isomerization in the absence of extra resources. Finally, we calculate two work quantities (Sec. IV): (i) the minimal work required for a light source to excite the molecule and (ii) the work extractable from the coherence in the molecule’s postisomerization state. Work can be extracted in case (ii) if molecules interact and obey indistinguishable-particle statistics. We conclude with this program’s significance and opportunities (Sec. V).

I. RESOURCE-THEORY MODEL FOR THE MOLECULAR SYSTEM

In this section, we review the resource theory that models heat exchanges. We then model the molecule, bath, light source, and photoisomerization process within the resource theory. To specify a system in the resource theory for heat exchanges, one specifies a tuple (ρ, H) .

The ρ denotes a quantum state, and the H denotes a Hamiltonian, defined on a dimension- d Hilbert space \mathcal{H} .

Each thermal operation consists of three steps: (i) A thermal system governed by an arbitrary Hamiltonian $H_{\mathcal{B}}$ is drawn from the bath at inverse temperature β : ($\rho_{\mathcal{B}} = \exp[-\beta H_{\mathcal{B}}]/Z_{\mathcal{B}}$, $H_{\mathcal{B}}$), wherein $Z_{\mathcal{B}} := \text{Tr}_{\mathcal{B}}[\exp(-\beta H_{\mathcal{B}})]$ denotes the partition function. (ii) The system and bath interact via an arbitrary energy-conserving unitary U . (iii) A generalized environment \mathcal{B}' is discarded. \mathcal{B}' is often the bath \mathcal{B} but may be another subsystem. Mathematically, a thermal operation \mathcal{T} is represented as

$$(\rho, H) \mapsto_{\text{TO}} \mathcal{T}(\rho, H) \equiv \left(\text{Tr}_{\mathcal{B}'} \{ U [\rho \otimes \rho_{\mathcal{B}}] U^\dagger \}, H \right), \quad (1)$$

wherein the unitary satisfies $[U, H + H_{\mathcal{B}}] = 0$. The Hamiltonians are composed as $H + H_{\mathcal{B}} \equiv (H \otimes \mathbb{1}) + (\mathbb{1} \otimes H_{\mathcal{B}})$. We do not assume any particular system-bath interaction U , and resource-theory results hold for arbitrarily large system-bath couplings. For concreteness, we restrict ourselves to an H representative of photoisomerization.

I A. Resource-theory model for the molecule, bath, and light source

The angular DOF $\varphi \in [0, \pi]$ parameterizes the isomer's configuration and governs the electronic Hamiltonian [18]. We attribute to the molecule the Hamiltonian

$$\begin{aligned} H_{\text{mol}} &:= \int_0^\pi d\varphi H_{\text{mol}}(\varphi) \\ &\equiv \int_0^\pi d\varphi \left[H_{\text{elec}}(\varphi) \otimes |\varphi\rangle\langle\varphi| + \mathbb{1}_{\text{elec}} \otimes \frac{\ell_\varphi^2}{2m} \right]. \end{aligned} \quad (2)$$

In each term in Eq. (2), the first factor acts on an electronic Hilbert space $\mathcal{H}_{\text{elec}}$, and the second acts on a configurational Hilbert space \mathcal{H}_φ . $\mathbb{1}_{\text{elec}}$ and $\mathbb{1}_\varphi$ denote the identity operators on $\mathcal{H}_{\text{elec}}$ and on \mathcal{H}_φ . We assume that φ is quasiclassical: The configuration's quantum state commutes with H_{mol} . The chemical groups' sizes and masses justify this assumption: The groups localize at angular coordinates far from the φ values at which $H_{\text{elec}}(\varphi)$ is degenerate, satisfying the Born-Oppenheimer approximation. ℓ_φ denotes the angular-momentum operator associated with the quasiclassical mode φ . The mode has an effective mass m .

Our H_{mol} has the form of Hamiltonians in [64, 69]. There, a switch changes the system-of-interest Hamiltonian. φ acts as the switch here, and the electronic DOF acts as the system.

The electronic Hamiltonian has the form in [18]:

$$\begin{aligned} H_{\text{elec}}(\varphi) &= \left[\frac{W_0}{2}(1 - \cos \varphi) \right] |\psi_0\rangle\langle\psi_0| \\ &+ \left[E_1 - \frac{W_1}{2}(1 - \cos \varphi) \right] |\psi_1\rangle\langle\psi_1| \\ &+ \frac{\lambda}{2} (|\psi_0\rangle\langle\psi_1| + |\psi_1\rangle\langle\psi_0|). \end{aligned} \quad (3)$$

The diabatic basis $\{|\psi_0\rangle, |\psi_1\rangle\}$ approximately diagonalizes the Hamiltonian at $\varphi = 0, \pi$. The constants $E_1, W_0, W_1 > 0$ far exceed the interstate coupling $\lambda > 0$. The vertical excitation energy from $|\psi_0\rangle|\varphi=0\rangle$ to $|\psi_1\rangle|\varphi=0\rangle$ is E_1 , and the energy stored during a transition from $|\psi_0\rangle|\varphi=0\rangle$ to $|\psi_0\rangle|\varphi=\pi\rangle$ is $\Delta E := E_1 - W_1$. Figure 1 shows this structure schematically. We notate the eigenenergies by $\mathcal{E}_\pm(\varphi)$, such that $\mathcal{E}_+(\varphi) \geq \mathcal{E}_-(\varphi)$, and the adiabatic basis by $\{|\mathcal{E}_\pm(\varphi)\rangle\}$:

$$H_{\text{elec}}(\varphi) = \sum_{\mu=\pm} \mathcal{E}_\mu(\varphi) |\mathcal{E}_\mu(\varphi)\rangle\langle\mathcal{E}_\mu(\varphi)|. \quad (4)$$

A Hamiltonian $H_{\mathcal{B}} = \sum_k \mathcal{E}_k |\mathcal{E}_k\rangle\langle\mathcal{E}_k|$ governs the bath, which occupies a Gibbs state $\rho_{\mathcal{B}} = \sum_k \exp(-\beta \mathcal{E}_k) / Z_{\mathcal{B}} |\mathcal{E}_k\rangle\langle\mathcal{E}_k|$. We assume that $H_{\mathcal{B}}$ has the properties in [64, Suppl. Note 1], e.g., degeneracies that scale exponentially with energy. We appeal to the justifications therein.

A laser or sunlight performs work on the molecule [68, 70–73]. We model the light as a multimode bosonic field in a state ρ_{laser} , e.g., a coherent state. An oscillator Hamiltonian

$$H_{\text{laser}} = \int_0^\infty \frac{d\omega}{2\pi} \hbar\omega \sum_{n_\omega=0}^\infty \left(|n_\omega\rangle\langle n_\omega| + \frac{\mathbb{1}}{2} \right) \quad (5)$$

governs the field. The particle-number states $|n_\omega\rangle$ satisfy the eigenvalue equation $N_\omega |n_\omega\rangle = n_\omega |n_\omega\rangle$, wherein $n_\omega = 0, 1, 2, \dots$. Each fixed- ω term resembles the ladder Hamiltonians with which batteries have been modeled in thermodynamic resource theories [66, 70, 74–76]. But the mathematically simplest resource-theory batteries have spectra unbounded from below, because ground states can complicate accountings of coherence [70, 77]. H_{laser} has a ground state, modeling a real physical Hamiltonian. But the ground state will lack much population.

I B. Resource-theory model for photoisomerization

The molecule begins thermalized with the bath, in the state $\rho = \exp(-\beta H_{\text{mol}}) / Z_{\text{mol}}$. We assume that Eq. 3 is parameterized such that the *cis* isomer is strongly energetically preferred: $\rho \approx |\psi_0\rangle\langle\psi_0| \otimes |\varphi=0\rangle\langle\varphi=0|$. We model photoisomerization with three thermal operations. First, the laser excites the molecule,

$$\begin{aligned} &e^{-\beta H_{\text{mol}}} / Z_{\text{mol}} \otimes |\varphi=0\rangle\langle\varphi=0| \otimes \rho_{\text{laser}} \\ &\mapsto_{\text{TO}} \rho_i \otimes |\varphi=0\rangle\langle\varphi=0|. \end{aligned} \quad (6)$$

at a fixed angular coordinate. ρ_i denotes the new electronic state. Second, the molecule rotates:

$$\rho_i \otimes |\varphi=0\rangle\langle\varphi=0| \mapsto_{\text{TO}} \rho_f \otimes |\varphi=\pi\rangle\langle\varphi=\pi|. \quad (7)$$

ρ_f denotes the post-photoisomerization state. Maximizing the isomerization yield amounts to maximizing the final state's weight on the lower *trans* level, $p_-(\pi) := \langle\mathcal{E}_-(\pi)|\rho_f|\mathcal{E}_-(\pi)\rangle$. In a more sophisticated model, the thermal operation (7) decomposes as a sequence of thermal operations. The angular DOF φ serves as a quantum clock [69, 70, 78–85] as the molecule rotates at some speed v . This sequence models a dissipative Landau-Zener transition and is detailed in the Appendix. Third, the molecule thermalizes to $\exp(-\beta H_{\text{mol}})/Z_{\text{mol}}$.

II. LIMITATIONS ON PHOTOISOMERIZATION YIELD

The rotational thermal operation (7) leaves the electronic DOF in a state ρ_f . We bound the optimal isomerization yield $\rho_-(\pi)$ via the resource-theory result of thermomajorization. By ‘‘optimal isomerization yield,’’ we mean the greatest value of $p_-(\pi)$ accessible after the preparation of ρ_i .

Thermomajorization is a preorder that constrains the populations' evolutions under thermal operations [61, 64, 86–92]. Let $H = \sum_{j=1}^d E_j |j\rangle\langle j|$ denote a Hamiltonian that governs a state ρ of energy diagonal $\mathcal{D}(\rho) := \sum_j |j\rangle\langle j| \rho |j\rangle\langle j| = \sum_j r_j |j\rangle\langle j|$. Consider rescaling the probabilities with Boltzmann factors, $r_j e^{\beta E_j}$, and ordering the products such that $r_{j'} e^{\beta E_{j'}} \geq r_{k'} e^{\beta E_{k'}}$ for all $j' > k'$. The convex hull of points $(\sum_{j'=1}^{\alpha} e^{-\beta E_{j'}}, \sum_{j'=1}^{\alpha} p_{j'})$, for all $\alpha = 1, 2, \dots, d$, defines a piecewise-linear curve. This Gibbs-rescaled Lorenz curve is denoted by $L_{(\rho, H)}(x)$, wherein the abscissa $x \in [0, Z]$ and $Z := \sum_{j=1}^d \exp(-\beta E_j)$. Let (σ, H) denote another system, represented by a Lorenz curve $L_{(\sigma, H)}(x)$. If the (ρ, H) curve lies above or on the (σ, H) curve at all $x \in [0, Z]$, we say that (ρ, H) thermomajorizes (σ, H) . If and only if (ρ, H) thermomajorizes (σ, H) does there exist a thermal operation that maps the first system's energy diagonal to the second system's:

$$L_{(\rho, H)}(x) \geq L_{(\sigma, H)}(x) \quad \forall x \in [0, Z] \quad \Leftrightarrow \quad (8) \\ \exists \mathcal{T} : \mathcal{T}(\mathcal{D}(\rho), H) = (\mathcal{D}(\sigma), H).$$

Relation (8) generalizes the second law of thermodynamics to arbitrarily small systems and to single shots.

The curve $L_{(\rho, H)}$ illustrates the thermodynamic value of (ρ, H) by codifying the system's informational and energetic resourcefulness. If the energies differ, r_j denotes the probability that measuring H will yield E_j . The more uniform $\{r_j\}$ is, the more uncertain the energy, and the less information ρ encodes. If the E_j 's equal

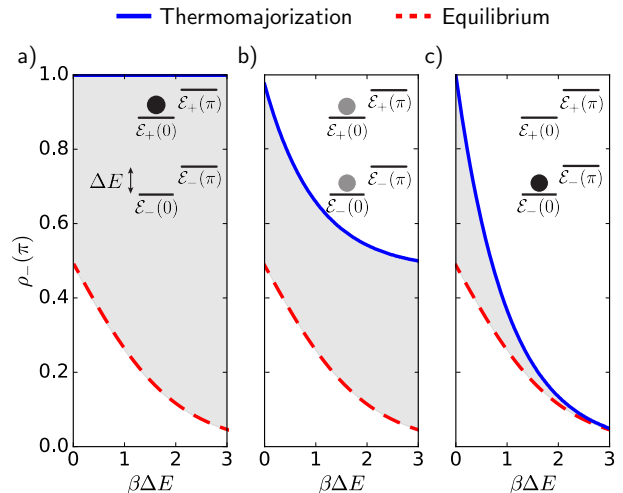


FIG. 2: Thermomajorization bound on the photoisomerization yield $\rho_-(\pi)$ and comparisons with equilibrium statistical mechanics. The red dashed curve shows the predicted equilibrium yield, and the blue solid curve shows the resource-theory bound. Possible optimal yields shown in the gray region from an initially excited state a), from an initial superposition b), and from an unexcited state c). The insets illustrate the molecule's energy levels. The shaded dots show the initial state's probability weights.

each other, $\{r_j\}$ equals the distribution over the degeneracies. In this case, $L_{(\rho, H)}$ illustrates the nonuniformity of $\{r_j\}$ in a way that no reduced measure, such as an entropy, can [61, 64, 65, 86–92]. In thermodynamics, not only information, but also energy, has value. Rescaling the probabilities r_j with the inverse Boltzmann factors $e^{\beta E_j}$ incorporates energetic resourcefulness into the information-theoretic $L_{(\rho, H)}$. These informational and energetic resources mirror the two terms in the Helmholtz free energy, $F = E - TS$. But the Helmholtz free energy characterizes average, equilibrium properties of large systems. Thermomajorization governs arbitrary nonequilibrium states of arbitrarily small systems.

II A. Thermomajorization bound

To bound the optimal photoisomerization yield $\rho_-(\pi)$, we construct the Gibbs-rescaled Lorenz curves for (i) the postexcitation state ρ_i and (ii) the post-rotation state ρ_f . We then solve for the greatest $\rho_-(\pi)$ that enables the photoexcited state to thermomajorize ρ_f :

$$L_{(\rho_i \otimes |\varphi=0\rangle\langle\varphi=0|, H_{\text{mol}})}(x) \\ \geq L_{(\rho_f \otimes |\varphi=\pi\rangle\langle\varphi=\pi|, H_{\text{mol}})}(x) \quad \forall x \in [0, Z_{\text{mol}}]. \quad (9)$$

In the following, we consider only two allowable angles, $\varphi = 0, \pi$, which define the *cis* and *trans* states. We assess how the bound depends on the *cis-trans* energy gap $\Delta E := \mathcal{E}_-(\pi) - \mathcal{E}_-(0)$, expressed in units of $1/\beta$. We

focus on the physically relevant regime in which $\Delta E \ll \mathcal{E}_+(0) - \mathcal{E}_-(0) =: E_1$.

Results are shown in Fig. 2 for three photoexcited states ρ_i . These states interpolate between the fully excited $|\psi_1\rangle|\varphi=0\rangle$, which can photoisomerize, to a $|\psi_0\rangle|\varphi=0\rangle$ that the laser has failed to excite. If the laser fails, only thermal excitations can isomerize the molecule. The resource-theory bound (9) is compared with the Boltzmann-factor yield predicted by equilibrium statistical mechanics, $\rho_-(\pi) = \exp[-\beta\mathcal{E}_-(\pi)]/Z_{\text{mol}}$. For all ρ_i , the equilibrium yield lies below the thermomajorization bound, as required. Moreover, the equilibrium yield lower-bounds the optimal yield, as any additional kinetic preference for converting *cis* to *trans* increases the yield, at least transiently. With thermomajorization upper-bounding possible outcomes, and equilibrium statistical mechanics lower-bounding them, we obtain a range of possible yields as a function of ρ_i and ΔE .

Suppose that the laser fully excites the molecule, to $\rho_i = |\mathcal{E}_+(0)\rangle\langle\mathcal{E}_+(0)|$. Thermomajorization caps the yield trivially at one, as shown in Fig. 2a). Hence energy conservation and the fixed-temperature bath do not limit the isomerization yield, in principle. The unboundedness persists across the range of physically reasonable gaps $\Delta E \ll E_1$. In contrast, as ΔE grows from the degeneracy point $\Delta E = 0$, the equilibrium estimate of the yield quickly decreases from 1/2. The equilibrium estimate vanishes as ΔE grows large, as expected from the Boltzmann distribution.

If the laser half-excites the molecule, such that $\mathcal{D}(\rho_i) = \frac{1}{2}|\mathcal{E}_+(0)\rangle\langle\mathcal{E}_+(0)| + \frac{1}{2}|\mathcal{E}_-(0)\rangle\langle\mathcal{E}_-(0)|$, the yield obeys the bounds in Fig. 2b). Rightward of the degeneracy point $\Delta E = 0$, the resource theory bound < 1 . As ΔE grows large, the bound approaches 1/2. The bound remains 1/2 for greater values of $\Delta E \ll E_1$. The equilibrium estimate is identical for all ρ_i , as, by construction, the estimate does not depend on the initial condition.

If the laser fails to excite the molecule, $\rho_i = |\mathcal{E}_-(0)\rangle\langle\mathcal{E}_-(0)|$. Thermal excitations drive the isomerization, whose bounds are shown in Fig. 2c). At large ΔE , the resource-theory bound asymptotes to 0. The bound approaches 1 as ΔE shrinks to 0.

Resource-theory insights explain several trends. If the laser fully excites the molecule, we saw, thermomajorization implies only that $\rho_-(\pi) \leq 1$. The reason follows from how, as reflected in $L_{(\rho, H)}$, thermodynamic resourcefulness decomposes into information and energy. The initial state is an energy eigenstate, $\rho_i = |\mathcal{E}_+(0)\rangle\langle\mathcal{E}_+(0)|$, so an energy measurement's outcome is perfectly predictable. ρ_i therefore encodes maximal information. ρ_i also has more energetic value than the lower *trans* state, as $E_1 > \Delta E$. Hence ρ_i has far more resourcefulness than $|\mathcal{E}_-(\pi)\rangle$. The fundamental thermodynamic limitations of energy conservation and temperature do not constrain the ability of ρ_i to transform into $|\mathcal{E}_-(\pi)\rangle$. Only kinetic practicalities, such relaxation rates do.

As probability weight shifts downward in ρ_i , ρ_i loses energetic value. ρ_i loses also informational value as $\mathcal{D}(\rho_i)$

grows more mixed. Hence the solid blue curve in Fig. 2b) lies below the solid blue curve in Fig. 2a). But the mixed $\mathcal{D}(\rho_i)$ retains significant energetic value, since $E_1 \gg \Delta E$. If the laser fails to excite the molecule, ρ_i regains informational value, being the energy eigenstate $|\mathcal{E}_-(0)\rangle\langle\mathcal{E}_-(0)|$. The dearth of energetic value outweighs this informational value, however.

II B. Kinetic factors that saturate bound

To gain insight into the factors that saturate the upper bounds, we consider a minimal kinetic model of relaxation following photoexcitation. We model the molecule's evolution with the Lindblad master equation

$$\dot{\rho}(t) = -\frac{i}{\hbar}[H, \rho(t)] + \mathcal{L}(\rho(t)). \quad (10)$$

The first term represents the system's coherent dynamics. Following the previous section, we consider only two angular states, so that the minimal Hamiltonian is $H \approx \sum_{\varphi=0, \pi} H_{\text{elec}}(\varphi)$ [Eq. (4)]. We set $\mathcal{E}_-(0) = 0$ and, as before, $\mathcal{E}_+(0) = E_1$ and $\mathcal{E}_-(\pi) = \Delta E$. For simplicity, we take $\mathcal{E}_+(\pi) = E_1 + \Delta E$, and we work in the physically relevant regime $E_1 \gg \Delta E > 0$. The levels' populations are denoted by $p_\mu(\varphi)$. The Lindblad equation's second term,

$$\mathcal{L}(\rho) = \sum_i \Gamma_i \left(B_i \rho B_i^\dagger - \frac{1}{2} \{ B_i^\dagger B_i, \rho(t) \} \right), \quad (11)$$

reflects the influence of the bath, which decoheres the state and dissipates energy. We choose Lindblad operators of the form $B_{\mathcal{E}_\mu(\varphi), \mathcal{E}_{\mu'}(\varphi')} = |\mathcal{E}_\mu(\varphi)\rangle\langle\mathcal{E}_{\mu'}(\varphi')|$, for each pair of energy eigenstates. Each B_i dissipates at a rate Γ_i assumed to satisfy local detailed balance,

$$\frac{\Gamma_{\mathcal{E}_\mu(\varphi), \mathcal{E}_{\mu'}(\varphi')}}{\Gamma_{\mathcal{E}_{\mu'}(\varphi'), \mathcal{E}_\mu(\varphi)}} = e^{-\beta[\mathcal{E}_\mu(\varphi) - \mathcal{E}_{\mu'}(\varphi')]}, \quad (12)$$

so the system relaxes toward a thermal state. To model the slowness of thermal isomerization, we set $\Gamma_{\mathcal{E}_-(0), \mathcal{E}_-(\pi)} = \Gamma_{\mathcal{E}_-(\pi), \mathcal{E}_-(0)} = 0$. Also processes involving the high-energy state $|\mathcal{E}_+(\pi)\rangle$ can be ignored.

This kinetic model sheds light on the resource-theory bound for the fully excited $\rho_i = |\mathcal{E}_+(0)\rangle\langle\mathcal{E}_+(0)|$. The Lindblad equation (10) can be solved analytically, though the result is a complicated expression. We can gain intuition from the regime

$$\Gamma_{\mathcal{E}_+(0), \mathcal{E}_-(\pi)} \gg \Gamma_{\mathcal{E}_+(0), \mathcal{E}_-(0)}, \quad (13)$$

in which relaxation into the *trans* state is kinetically preferred. Furthermore, satisfying Ineq. (13) and

$$E_1 \gg \Delta E \quad (14)$$

simultaneously enables the Lindblad evolution to saturate the resource-theory bounds, as we shall see. Under

Ineq. (13), the ground *trans* state has a population of

$$\rho_-(\pi) = \frac{1}{1 + e^{\beta(\Delta E - E_1)}} (1 - e^{-tk}) \quad (15)$$

at early times $t \ll 1/\Gamma_{\mathcal{E}_+(0),\mathcal{E}_-(0)}$. The population grows, from 0 at $t = 0$, with the effective rate $k = \Gamma_{\mathcal{E}_+(0),\mathcal{E}_-(\pi)} + \Gamma_{\mathcal{E}_-(\pi),\mathcal{E}_+(0)}$. This evolution is shown in Fig. 3a), where $\beta\Delta E = 1.5$, $\beta E_1 = 30$, $\beta\hbar\Gamma_{\mathcal{E}_+(0),\mathcal{E}_-(\pi)} = 1$, and $\beta\hbar\Gamma_{\mathcal{E}_+(0),\mathcal{E}_-(0)}/\beta\hbar\Gamma_{\mathcal{E}_+(\pi),\mathcal{E}_+(0)} = 0.01$. The values do not affect the qualitative results, so long as the constants satisfy Ineqs. (13) and (14). In the intermediate-time limit, $1/\Gamma_{\mathcal{E}_+(0),\mathcal{E}_-(0)} \gg t \gg 1/k$, the molecule likely isomerizes: $\rho_-(\pi)$ approaches 1.

If the molecule's probability weight is initially spread evenly, $\rho_i = \frac{1}{2}|\mathcal{E}_+(0)\rangle\langle\mathcal{E}_+(0)| + \frac{1}{2}|\mathcal{E}_-(0)\rangle\langle\mathcal{E}_-(0)|$, the Lindblad evolution leads to Fig. 3b). We have reused the parameters in Fig. 3a). Again, Inequalities (13) and (14) saturate the resource-theory bound at intermediate times. But here, the bound reaches only 1/2.

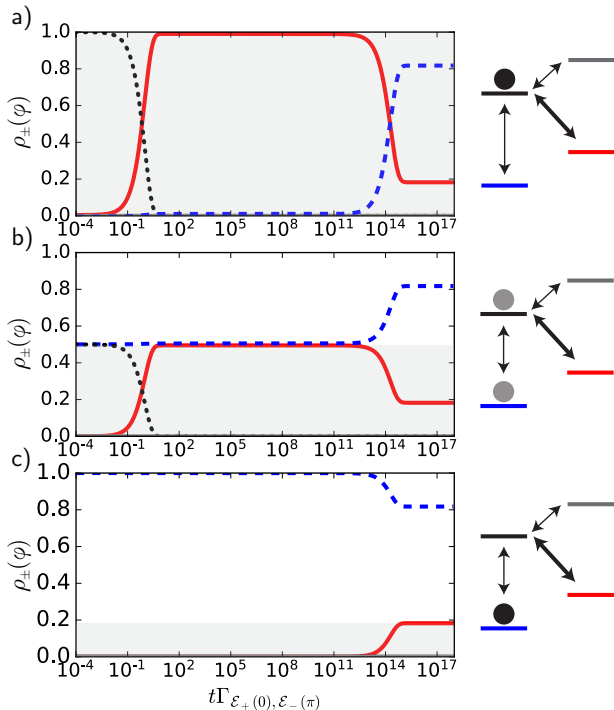


FIG. 3: Comparison of thermomajorization bound with time-dependent Lindblad dynamics. Calculations are performed on the four-level system shown on the right. The filled circles illustrate the initial probability weights, and the arrows signify the possible transitions. Each energy level's population evolves as the correspondingly colored curves in the plots: $|\mathcal{E}_+(0)\rangle$ (dotted black), $|\mathcal{E}_-(\pi)\rangle$ (solid red), $|\mathcal{E}_-(0)\rangle$ (dashed blue), and $|\mathcal{E}_+(\pi)\rangle$ (solid gray). The grayed area denotes the region accessible to $|\mathcal{E}_-(\pi)\rangle$ according to thermomajorization. Population dynamics are shown following a) full excitation to $|\mathcal{E}_+(0)\rangle$, b) half-excitation to a state of energy diagonal $\frac{1}{2}|\mathcal{E}_+(0)\rangle\langle\mathcal{E}_+(0)| + \frac{1}{2}|\mathcal{E}_-(0)\rangle\langle\mathcal{E}_-(0)|$, and c) failure to excite the state above $|\mathcal{E}_-(0)\rangle$.

long times, the yield approaches its equilibrium value, as in Fig. 3a).

Figure 3c) reflects a molecule that the laser has failed to excite: $\rho_i = |\mathcal{E}_-(0)\rangle\langle\mathcal{E}_-(0)|$. Isomerization results from equilibrium fluctuations that delocalize ρ_i into a mixture of *cis* and *trans* states. The yield maximizes, reaching the resource-theory bound, at very long times set by the large barrier in the ground electronic state $\mathcal{E}_-(\varphi)$.

III. LIMITATIONS ON COHERENCE FOLLOWING PHOTOISOMERIZATION

So far, we have focused on energy-eigenstate populations. But photoexcitation may inject coherence into the molecule's state. By “coherence,” we mean, here, coherence relative to the energy eigenbasis. Such coherence may contribute dynamically to the thermal relaxation's outcome. Using the resource-theory tool of monotones, we bound the amount of coherence in ρ_f . Though excitation may create coherence in the electronic state, we argue that this coherence cannot increase the isomerization yield in the absence of extra resources.

III A. Independence of coherence modes

A monotone is a function f , evaluated on a system (ρ, H) , that decreases monotonically under free operations [48, 65, 92]: $f(\rho, H) \geq f(\mathcal{T}(\rho, H))$. Monotones quantify resourcefulness, which free operations, i.e., thermalization, preserve or erode. Different monotones quantify the system's ability to fuel different tasks, such as work extraction and timekeeping.

Coherence can be grouped into modes, each associated with one energy gap [71, 93]. Let $H = \sum_j E_j |j\rangle\langle j|$ denote a Hamiltonian that governs a state ρ . The ω mode of H consists of the pairs (j, k) whose gaps $|E_j - E_k| = \omega$. If $\rho_{jk} := \langle j|\rho|k\rangle$, then ρ_{jk} encodes coherence when $j \neq k$. A state's mode- ω coherence has been quantified with the one-norm [71], defined as $\|A\|_1 := \text{Tr}(\sqrt{AA^\dagger})$ for a matrix A . Suppose that some thermal operation \mathcal{T} maps (ρ, H) to (σ, H) . The modes' one-norms decay monotonically and independently [71]:

$$\sum_{j,k:|E_j-E_k|=\omega} \|\rho_{jk}\|_1 \geq \sum_{j,k:|E_j-E_k|=\omega} \|\sigma_{jk}\|_1 \quad \forall \omega. \quad (16)$$

The molecule's $H_{\text{elec}}(0)$ has a coherence mode $\omega_1 = \mathcal{E}_+(0) - \mathcal{E}_-(0) = E_1$ and a population mode $\omega_0 = 0$. The initial state $\approx |\mathcal{E}_-(0)\rangle$ lacks coherence, so the laser provides all the coherence in the photoexcited state ρ_i . Suppose that the laser creates an even superposition, $\frac{1}{\sqrt{2}}(|\mathcal{E}_-(0)\rangle + |\mathcal{E}_+(0)\rangle)|\varphi=0\rangle$, as in Fig. 2b). Photoex-

citation gives the state a nonzero amount

$$\left\| \sum_{(j,k)=(+,-),(-,+)} (\rho_i)_{jk} \right\|_1 = 1 \quad (17)$$

of coherence. Since modes transform independently under thermal operations, the ω_1 coherence cannot influence the ω_0 populations. If the target *trans* state is an energy eigenstate, therefore, injecting coherence via photoexcitation cannot improve the isomerization yield in the absence of extra resources.

III B. Fisher-information monotone

Focusing on $\varphi = 0, \pi$, we upper-bounded the isomerization yield $\rho_-(\pi)$ (Sec. II A). But we might wish to calculate $\rho_-(\pi)$, using resource-theory tools. We must model the full rotation, $\varphi \in [0, \pi]$, within the resource theory. We do so in the appendix, treating φ as a quantum clock [69, 70, 78–85]. The chemical groups' angular momentum, ℓ_φ , governs the rotation speed. To illustrate how the momentum can affect the dynamics, we here linearize $H_{\text{elec}}(\varphi)$ near the avoiding crossing point at $\varphi = \cos^{-1} \left(\frac{W_0 + W_1 - 2E_1}{W_0 + W_1} \right)$. For simplicity, we assume that the momentum remains constant.

The resulting Hamiltonian has the form of a Landau-Zener (LZ) model,

$$H_{\text{LZ}}(t) \approx -vt (|\psi_1\rangle\langle\psi_1| - |\psi_0\rangle\langle\psi_0|) + \frac{\lambda}{2} (|\psi_0\rangle\langle\psi_1| + \text{h.c.}) \quad (18)$$

illustrated near the crossing point in Fig. 1. The Hamiltonian changes at a speed $v \propto |d\varphi/dt|$ that has dimensions of energy/time. The time, t , runs from $-\infty$ to ∞ in the Landau-Zener model. Suppose that the molecule begins in the upper diabatic level, $|\psi_1\rangle$. If $v \ll \lambda^2/\hbar$, the state evolves adiabatically, changing from $|\psi_1\rangle$ but remaining in the upper instantaneous eigenstate. If $v \gg \lambda^2/\hbar$, the state evolves diabatically, remaining (approximately) $|\psi_1\rangle$, which becomes approximately the lower energy eigenstate. Isomerization in the presence of a thermal bath amounts to a dissipative LZ transition[94–97]. We model the transition within the resource theory in the appendix. Here, we quantify the postisomerization coherence with the quantum Fisher information I_F relative to the Hamiltonian, a resource-theory monotone [98].

I_F quantifies mixed and pure states' coherences [98, 99]. Let ρ denote a quantum state that eigendecomposes as $\rho = \sum_j r_j |j\rangle\langle j|$. The Fisher information with respect to a Hamiltonian H is

$$I_F(\rho, H) = 2 \sum_{j,k} \frac{(r_j - r_k)^2}{r_j + r_k} |\langle j|H|k\rangle|^2. \quad (19)$$

I_F quantifies the state's ability to distinguish instants as a quantum clock [98]. When evaluated on a pure state

$\rho = |\chi\rangle\langle\chi|$, I_F reduces to four times the energy variance, $\langle H^2 \rangle - \langle H \rangle^2$.

We can calculate explicitly the Fisher information of $\rho_f = \sum_{i,j=0,1} \rho_{ij} |\psi_i\rangle\langle\psi_j|$. For the Landau-Zener Hamiltonian,

$$I_F(\rho_f, H_{\text{LZ}}(t_f)) = \lambda^2 \left| 1 - 2\rho_{00} - 4 \frac{vt_f}{\lambda} \text{Re}(\rho_{01}) \right|^2, \quad (20)$$

wherein the density matrix and the Hamiltonian are evaluated at $t = t_f \gg \lambda/v$. The gap, λ , sets the distance tuned through in energy space, due to (i) the Hamiltonian's linearization and (ii) the order-one change in the angle, π . We have invoked the state's normalization, $\rho_{00} + \rho_{11} = 1$. Consider the long-time limit, and suppose that $\rho_{01} \neq 0$. The term proportional to vt_f dominates Eq. (20), and

$$I_F \sim 16v^2 t_f^2 |\text{Re}(\rho_{01})|^2. \quad (21)$$

The simplified I_F depends on the off-diagonal elements of the density matrix relative to the diabatic basis. Furthermore, this I_F is proportional to the momentum squared. This proportionality quantifies how underdamping near the avoided crossing generates more coherence than overdamping would generate. Since I_F is a monotone, evaluating it for a closed system upper-bounds the coherence generated in the presence of a thermal bath. The long-time population is well-approximated by the Landau-Zener transition probability, $\rho_{11} \approx \exp\left(-\frac{\pi\lambda^2}{2\hbar v}\right)$ [44]. We approximate the long-time density matrix's off-diagonal elements by neglecting the phase: $\rho_{01} \approx \exp\left(-\frac{\pi\lambda^2}{4\hbar v}\right) \sqrt{1 - \exp\left(-\frac{\pi\lambda^2}{2\hbar v}\right)}$. Within the approximate treatment of the avoided crossing, therefore, the final-state coherence is upper-bounded by

$$I_F^+ = 16v^2 t_f^2 e^{-\pi\lambda^2/(2\hbar v)} \left(1 - e^{-\pi\lambda^2/(2\hbar v)}\right). \quad (22)$$

Any action of the bath results in

$$I_F(\rho_f, H_{\text{LZ}}(t_f)) < I_F^+, \quad (23)$$

since I_F is a resource theory monotone.

III C. Dissipative Landau-Zener transition

To study the bath's effects on the Landau-Zener evolution of the coherences, we have evaluated I_F on the molecule's post-rotation state, ρ_f , using a Lindblad master equation analogous to Eq. 10. The system Hamiltonian H has the approximate Landau-Zener form $H_{\text{LZ}}(t)$. We suppose that the system couples to the bath through the operator

$$B = |\psi_1\rangle\langle\psi_1| - |\psi_0\rangle\langle\psi_0|. \quad (24)$$

The operator's key feature is that, relative to the $H_{\text{LZ}}(t)$ eigenbasis near the avoided crossing, B is represented by

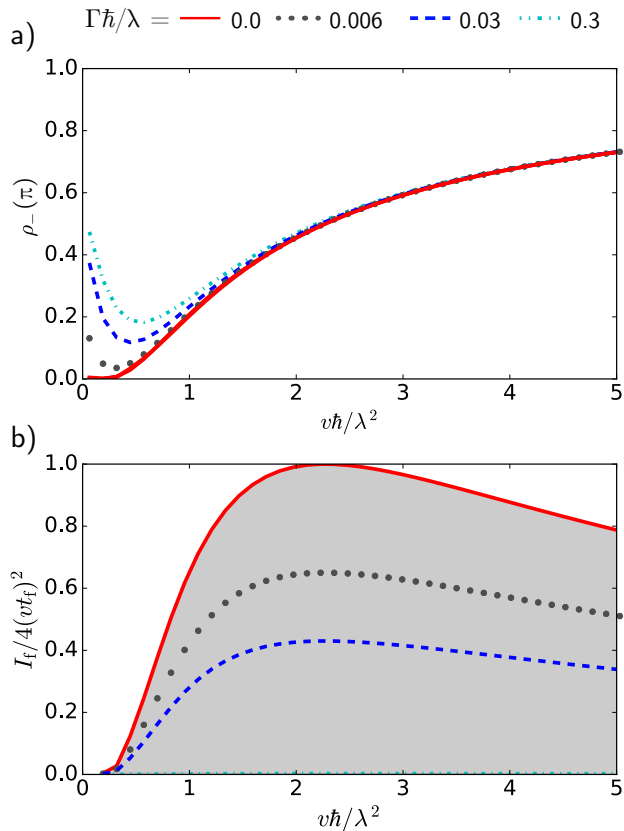


FIG. 4: Dissipative Landau-Zener model for the lower *trans* state’s population and for coherence. The initial state, $|\psi_1\rangle$, was evolved from an initial time of $-t_f$ to $t_f = 50\hbar/\lambda$. a) Final lower-*trans*-level population as a function of transition speed, v , for different dephasing rates Γ . b) Reduced Fisher information, as a function of v for different dephasing rates Γ . The grayed area represents the monotone bound (23).

a nondiagonal matrix. The off-diagonal elements enable B to transfer population between energy levels. B decoheres the state at a rate Γ . To obtain ρ_f , we prepared the electronic state $|\psi_1\rangle$ and simulated evolution from times $t = -t_f$ to $t_f = 50\hbar/\lambda$. For simplicity, we adopt a unit system in which $\lambda = \hbar = 1$. We focus on the dependences on v and Γ .

Figure 4a) shows the photoisomerization yields, under Landau-Zener dynamics, for different decoherence rates. If $\Gamma = 0$, the yield is well-described by the canonical Landau-Zener transition probability $\rho_{-}(\pi) = \rho_{11} \approx \exp\left(-\frac{\pi\lambda^2}{2\hbar v}\right)$. At low speeds, $v\hbar/\lambda^2 \ll 1$, the yield is small. The system evolves adiabatically, ending in the diabatic state $|\psi_0\rangle$. At high speeds, $v\hbar/\lambda^2 \gg 1$, the yield is greater: The system has no time to transition to $|\psi_0\rangle$ and so remains in $|\psi_1\rangle$.

Consider raising the phase-damping rate Γ at a fixed v . If the speed is low, $v\hbar/\lambda^2 \ll 1$, the yield rises. If the speed is large, $v/\lambda \gg \Gamma$, the yield about equals its

decoherence-free value, regardless of Γ . The yield minimizes when $\Gamma \approx v/\lambda$: The decoherence’s mixing of energy eigenstates, which transfers about half the state’s weight to the lower energy level, balances adiabaticity’s preservation of the upper level’s weight. Similar behavior was observed in [96]. Whereas earlier work focused on the populations, we quantify how the coherences evolve in the dissipative Landau-Zener problem.

Figure. 4b) shows the Fisher information scaled by $1/(4v^2t_f^2)$. When $\Gamma = 0$, I_f adheres to the asymptotic prediction I_f^+ [Eq. (22)], represented by the grayed region. The asymptotic bound (23) limits the coherence, we verified, for finite Γ . Raising Γ above 0 decreases the scaled Fisher information toward 0.

The scaled coherence peaks at an intermediate speed given by Eq. (22). At this v , half the population transitions from the initial excited state, $|\psi_1\rangle$, to the final ground state, $|\psi_1\rangle$. Transitioning half the population spreads probability weight evenly across the energy levels. Even spreading accompanies maximal coherence. This observation agrees with the quantum adiabatic theorem: If $H_{LZ}(t)$ changes slowly, the electronic DOF remains in an instantaneous energy eigenstate. The final state, $|\mathcal{E}_+(\pi)\rangle$, therefore lacks coherence. If $H_{LZ}(t)$ changes quickly, the state has no time evolve away from $|\psi_1\rangle$. Since $|\psi_1\rangle$ becomes the $H_{LZ}(t_f)$ ground level, the final state again lacks coherence. Hence low and high v ’s lead to small coherences that we have quantified with $I_f/(4v^2t_f^2)$.

In summary, isomerization partially trades off with coherence. Little population transfer, which is undesirable, accompanies little coherence. Little coherence accompanies also a desirable large population transfer. Midsized population transfer accompanies large coherences. We have quantified these trends with the Fisher information. Moreover, we conclude, coherence does not straightforwardly promote isomerization in this minimal model.

IV. WORK INJECTION AND EXTRACTION

Using the resource-theory framework, we calculate the minimal amount of work required to photoexcite the molecule. We also find that work can be extracted from postisomerization coherence, if molecules interact and obey indistinguishable-particle statistics. We use two resource-theory tools: (i) one-shot information theory, which generalizes Shannon information theory to small scales, and (ii) quantum-thermodynamic results about extracting work from coherence.

IV A. Minimal work required to photoisomerize

How much work must one invest to excite a molecule from $|\psi_0\rangle|\varphi=0\rangle \approx \exp(-\beta H_{\text{mol}})/Z_{\text{mol}}$ to $|\psi_1\rangle|\varphi=0\rangle$? One might expect an average of about $\mathcal{E}_+(0) - \mathcal{E}_-(0)$.

But the single-photon limit invites us to consider the minimal work W_{\min} required in any one shot. One-shot work can be calculated with thermodynamic resource theories [64, 76, 91, 100–103]. Calculations rely on one-shot information theory [104–108], which extends Shannon information theory [109] to small scales and few trials.

Work is defined, in thermodynamic resource theories, in terms of a battery [64]. The battery can manifest as an oscillator governed by a Hamiltonian like one term in Eq. (5) [66, 70, 74, 76]. A battery performs work while facilitating a system-of-interest transformation from some state ρ to some state ρ' . The work is positive, $\hbar\omega > 0$ if the battery de-excites: $(\rho \otimes |n_\omega\rangle\langle n_\omega|) \mapsto_{\text{TO}} (\rho' \otimes |n_\omega - 1\rangle\langle n_\omega - 1|)$. We regard the light source as consisting of batteries of various gaps $\hbar\omega$ (see Sec. I A).

Consider creating one copy of an arbitrary energy-diagonal system $(\mathcal{D}(\rho), H)$ from a thermal system $(\exp[-\beta H]/Z, H)$. The minimal work required has been shown to equal

$$W_{\min}(\mathcal{D}(\rho), H) = \frac{1}{\beta} D_{\max}(\rho || e^{-\beta H}/Z) \quad (25)$$

[64]. The max relative entropy between quantum states ρ and σ is defined as

$$D_{\max}(\rho || \sigma) := \log(\min\{c \in \mathbb{R} : \rho \leq c\sigma\}). \quad (26)$$

We set logarithms to be base- e in this paper. D_{\max} is well-defined if the first state's support lies in the second state's: $\text{supp}(\rho) \subseteq \text{supp}(\sigma)$.

Let us evaluate these expressions on $|\psi_1\rangle|\varphi=0\rangle$. We notate the energy diagonal as

$$\begin{aligned} \mathcal{D}(|\psi_1\rangle\langle\psi_1| \otimes |\varphi=0\rangle\langle\varphi=0|) \\ = \sum_{\mu=\pm} p_\mu |\mathcal{E}_\mu(0)\rangle\langle\mathcal{E}_\mu(0)| \otimes |\varphi=0\rangle\langle\varphi=0|. \end{aligned} \quad (27)$$

Substituting into Eq. (25) yields

$$\begin{aligned} W_{\min}(\mathcal{D}(|\psi_1\rangle\langle\psi_1| \otimes |\varphi=0\rangle\langle\varphi=0|), H_{\text{mol}}) \\ = \min \left\{ \mathcal{E}_+(0) - \frac{1}{\beta} \log(1/p_+), \mathcal{E}_-(0) - \frac{1}{\beta} \log(1/p_-) \right\} \\ - \left(-\frac{1}{\beta} \log Z_{\text{mol}} \right). \end{aligned} \quad (28)$$

Each entry in the $\{\dots\}$ equals a one-shot variation on a free-energy difference: The Helmholtz free energy is $F := E - TS$. The eigenenergy $\mathcal{E}_\pm(0)$ replaces the average energy E . p_\pm equals a probability, so $-\log(p_\pm)$ equals a surprisal: Consider preparing $|\psi_1\rangle$, then measuring $\{|\mathcal{E}_\pm\rangle\}$. The surprisal quantifies the information you gain, or the surprise you register, upon learning the outcome. Averaging the surprisal over many trials yields the Shannon entropy, $S_{\text{Sh}} = -\sum_{\mu=\pm} p_\mu \log p_\mu$. The Shannon entropy is proportional to the thermodynamic entropy S , for equilibrium states. Hence the $-\frac{1}{\beta} \log(1/p_\pm)$ is a one-shot variation on the $-TS$ in F . The equilibrium state $\exp(-\beta H_{\text{mol}})/Z_{\text{mol}}$ has a free energy of

$F = -\frac{1}{\beta} \log Z_{\text{mol}}$. Hence the minimal one-shot work has the form (one-shot nonequilibrium free energy) - (equilibrium free energy).

IV B. Extracting work from postisomerization coherence

The postisomerization state ρ_f can have coherence between unequal-energy levels, $|\mathcal{E}_\pm(\pi)\rangle|\varphi=\pi\rangle$. Work can be extracted from coherence between degenerate levels, resource-theory results show [74, 98, 110, 111]. We can generate degenerate-level coherence from unequal-energy coherence, using multiple copies of the system. The work comes from coherence because the extraction preserves the state's energy diagonal.

Consider two molecules that dissipate weakly during isomerization. Having begun in a nearly pure state, the isomers end nearly in some pure state $|\chi\rangle|\varphi=\pi\rangle^{\otimes 2}$. The electronic factor has the form

$$\begin{aligned} |\chi\rangle = \sqrt{p_{--}} |\mathcal{E}_-(\pi), \mathcal{E}_-(\pi)\rangle + \sqrt{p_{-+}} |\mathcal{E}_-(\pi), \mathcal{E}_+(\pi)\rangle \\ + \sqrt{p_{+-}} |\mathcal{E}_+(\pi), \mathcal{E}_-(\pi)\rangle + \sqrt{p_{++}} |\mathcal{E}_+(\pi), \mathcal{E}_+(\pi)\rangle. \end{aligned} \quad (29)$$

One can initiate work extraction by measuring the system's energy, e.g., to ascertain how much work is expected and so to guide instrument calibration. Suppose that (i) the equal-energy eigenstates have equal prefactors, $\sqrt{p_{-+}} = \sqrt{p_{+-}}$, and (ii) the greatest Gibbs-rescaled probability is p_{+-} :

$$\arg \max_{\mathcal{E}} \left\{ p_{\mu\nu} e^{\beta \mathcal{E}} \right\} = \mathcal{E}_+(\pi) + \mathcal{E}_-(\pi). \quad (30)$$

Suppose, further, that the measurement yields the degenerate energy, $\mathcal{E}_-(\pi) + \mathcal{E}_+(\pi)$. The system is projected onto a pure state, $\frac{1}{\sqrt{2}} [|\mathcal{E}_-(\pi), \mathcal{E}_+(\pi)\rangle + |\mathcal{E}_+(\pi), \mathcal{E}_-(\pi)\rangle]$, in a two-dimensional space. The pure state has more informational value than the same-energy-diagonal mixed state, $\frac{1}{2} [|\mathcal{E}_-(\pi)\rangle\langle\mathcal{E}_-(\pi)| + |\mathcal{E}_+(\pi)\rangle\langle\mathcal{E}_+(\pi)|]$. The pure state can be decohered to the mixed state while the extra value is extracted as work (see Fig. 2 in [98]).

Let us illustrate how a two-molecule state can satisfy the criterion (30). Though artificial, the illustration demonstrates achievability. Suppose that the molecules occupy a small, symmetric structure. Their real-space wave functions might overlap considerably, rendering the molecules indistinguishable [112]. The molecules would occupy a symmetric or an antisymmetric state, depending on their total spins [112]. Hence the electronic DOFs could occupy an antisymmetric state [112]. Suppose that a Heisenberg Hamiltonian $(\text{const.}) \boldsymbol{\sigma} \cdot \boldsymbol{\sigma}$ couples the electronic DOFs, which thermalize with a $T = 0$ bath. Let the Hamiltonian's proportionality constant be positive. The electronic state becomes the singlet $\frac{1}{\sqrt{2}}(|01\rangle - |10\rangle)$, satisfying Eq. (30). Work can therefore be extracted from the state's coherence.

V. OUTLOOK

We have bounded fundamental limitations on photoisomerization, using thermodynamic resource theories. The bounds are simple, general, and derived from few assumptions. Yet the results shed light on the roles played by information, energy, and coherence in molecules prevalent in natural and artificial materials.

Similar insights may follow from modeling other chemical systems with thermodynamic resource theories. Candidates include chlorophyll [113–116] and photovoltaics [117–120]. Exciton transport there may be bounded as isomerization is here. Additionally, azobenzene has been attached to carbon nanotubes [28]. The attachment raised the isomers’ capacity for storing solar fuel by 200%, though 30% was expected. The improvements achievable—and the engineering effort exerted—might be upper-bounded with a variation on our model.

This work leverages resource theories, which have remained largely abstract, to solve known problems in experimental systems. A bridge for thermodynamic resource theories from mathematical physics to the real physical world was called for recently [121]; construction has just begun [72, 122–124]. Experimental proposals designed to realize resource-theory results have provided a valuable first step. The present paper progresses from artifice to explaining diverse phenomena realized already in nature and in experiments. This program may be advanced through this paper’s resource-theory model for Landau-Zener transitions, as such transitions occur throughout chemistry and many-body physics.

ACKNOWLEDGMENTS

NYH thanks Bassam Helou, David Jennings, Christopher Perry, and Mischa Woods for conversations. NYH is grateful for funding from the Institute for Quantum Information and Matter, an NSF Physics Frontiers Center (NSF Grant PHY-1125565) with support from the Gordon and Betty Moore Foundation (GBMF-2644), for a Barbara Groce Graduate Fellowship, for a KITP Graduate Fellowship (the KITP receives support from the NSF under Grant No. NSF PHY-1125915), and for an NSF grant for the Institute for Theoretical Atomic, Molecular, and Optical Physics at Harvard University and the Smithsonian Astrophysical Observatory. DTL was supported by UC Berkeley College of Chemistry and by the Kavli Energy NanoSciences Institute.

REFERENCES

[1] C. Jarzynski, *Physical Review Letters* **78**, 2690 (1997).
 [2] G. E. Crooks, *Physical Review E* **60**, 2721 (1999).
 [3] R. Klages, W. Just, and C. Jarzynski, *Nonequilibrium statistical physics of small systems: Fluctuation relations and beyond* (John Wiley & Sons, 2013).

[4] D. Collin *et al.*, *Nature* **437**, 231 (2005).
 [5] E. Trepagnier *et al.*, *Proceedings of the National Academy of Sciences* **101**, 15038 (2004).
 [6] D. Mandal and C. Jarzynski, *Proceedings of the National Academy of Sciences* **109**, 11641 (2012).
 [7] S. Toyabe, T. Sagawa, M. Ueda, E. Muneyuki, and M. Sano, *Nature physics* **6**, 988 (2010).
 [8] J. V. Koski, V. F. Maisi, T. Sagawa, and J. P. Pekola, *Physical review letters* **113**, 030601 (2014).
 [9] A. C. Barato and U. Seifert, *Physical review letters* **114**, 158101 (2015).
 [10] T. R. Gingrich, J. M. Horowitz, N. Perunov, and J. L. England, *Physical review letters* **116**, 120601 (2016).
 [11] A. C. Barato, D. Hartich, and U. Seifert, *New Journal of Physics* **16**, 103024 (2014).
 [12] A. C. Barato and U. Seifert, *Physical Review X* **6**, 041053 (2016).
 [13] M. Nguyen and S. Vaikuntanathan, *Proceedings of the National Academy of Sciences* **113**, 14231 (2016).
 [14] R. Marsland III and J. England, *Reports on Progress in Physics* **81**, 016601 (2017).
 [15] D. H. Waldeck, *Chemical Reviews* **91**, 415 (1991).
 [16] H. D. Bandara and S. C. Burdette, *Chemical Society Reviews* **41**, 1809 (2012).
 [17] S. Hahn and G. Stock, *The Journal of Physical Chemistry B* **104**, 1146 (2000).
 [18] S. Hahn and G. Stock, *The Journal of Chemical Physics* **116**, 1085 (2002), <https://doi.org/10.1063/1.1428344>.
 [19] W. R. Browne and B. L. Feringa, *Nature Nanotechnology* **1**, 25 (2006).
 [20] B. G. Levine and T. J. Martínez, *Annu. Rev. Phys. Chem.* **58**, 613 (2007).
 [21] O. Strauss, *Physiological reviews* **85**, 845 (2005).
 [22] R. Y. Tsien, *Annu. Rev. Biochem* **67**, 509 (1998).
 [23] G. Vogt, G. Krampert, P. Niklaus, P. Nuernberger, and G. Gerber, *Phys. Rev. Lett.* **94**, 068305 (2005).
 [24] G. Vogt *et al.*, *Phys. Rev. A* **74**, 033413 (2006).
 [25] C. Brif, R. Chakrabarti, and H. Rabitz, *New Journal of Physics* **12**, 075008 (2010).
 [26] V. I. Prokhorenko *et al.*, *science* **313**, 1257 (2006).
 [27] C. Arango and P. Brumer, *The Journal of Chemical Physics* **138**, 071104 (2013).
 [28] T. J. Kucharski *et al.*, *Nature Chemistry* **6**, 441 (2014).
 [29] T. J. Kucharski *et al.*, *Nature chemistry* **6**, 441 (2014).
 [30] Y. Zhao and T. Ikeda, *Smart light-responsive materials: azobenzene-containing polymers and liquid crystals* (John Wiley & Sons, 2009).
 [31] A. H. Zewail, *The Journal of Physical Chemistry* **100**, 12701 (1996).
 [32] S. Mukamel, *Annual review of physical chemistry* **51**, 691 (2000).
 [33] D. M. Jonas, *Annual review of physical chemistry* **54**, 425 (2003).
 [34] T. A. Oliver, N. H. Lewis, and G. R. Fleming, *Proceedings of the National Academy of Sciences* , 201409207 (2014).
 [35] D. A. Micha, *The Journal of Chemical Physics* **137**, 22A521 (2012).
 [36] A. Kelly and T. E. Markland, *The Journal of Chemical Physics* **139**, 014104 (2013).
 [37] A. Montoya-Castillo, T. C. Berkelbach, and D. R. Reichman, *The Journal of Chemical Physics* **143**, 194108 (2015).
 [38] W. H. Miller, *The Journal of Chemical Physics* **53**, 3578

- (1970).
- [39] M. Ben-Nun and T. J. Martínez, *The Journal of Chemical Physics* **108**, 7244 (1998).
- [40] M. Topaler and N. Makri, *The Journal of Physical Chemistry* **100**, 4430 (1996).
- [41] R. Kapral and G. Ciccotti, *The Journal of Chemical Physics* **110**, 8919 (1999).
- [42] A. McLachlan, *Molecular Physics* **8**, 39 (1964).
- [43] J. C. Tully, *The Journal of Chemical Physics* **93**, 1061 (1990).
- [44] A. Nitzan, *Chemical dynamics in condensed phases: relaxation, transfer and reactions in condensed molecular systems* (Oxford university press, 2006).
- [45] J. C. Tully, *The Journal of Chemical Physics* **137**, 22A301 (2012).
- [46] A. J. Schile and D. T. Limmer, arXiv:1809.03501 (2018).
- [47] B. Coecke, T. Fritz, and R. W. Spekkens, *Information and Computation* **250**, 59 (2016), *Quantum Physics and Logic*.
- [48] E. Chitambar and G. Gour, ArXiv e-prints (2018), 1806.06107.
- [49] R. Horodecki, P. Horodecki, M. Horodecki, and K. Horodecki, *Rev. Mod. Phys.* **81**, 865 (2009).
- [50] S. J. van Enk, *Phys. Rev. A* **71**, 032339 (2005).
- [51] J. A. Vaccaro, F. Anselmi, H. M. Wiseman, and K. Jacobs, *Phys. Rev. A* **77**, 032114 (2008).
- [52] S. D. Bartlett, T. Rudolph, R. W. Spekkens, and P. S. Turner, *New J. Phys.* **8**, 58 (2006).
- [53] S. D. Bartlett, T. Rudolph, and R. W. Spekkens, *Rev. Mod. Phys.* **79**, 555 (2007).
- [54] G. Gour and R. W. Spekkens, *New Journal of Physics* **10**, 033023 (2008).
- [55] I. Marvian and R. W. Spekkens, *New Journal of Physics* **15**, 033001 (2013).
- [56] T. Baumgratz, M. Cramer, and M. B. Plenio, *Phys. Rev. Lett.* **113**, 140401 (2014).
- [57] A. Winter and D. Yang, *Phys. Rev. Lett.* **116**, 120404 (2016).
- [58] E. Chitambar and G. Gour, *Phys. Rev. Lett.* **117**, 030401 (2016).
- [59] V. Veitch, S. A. H. Mousavian, D. Gottesman, and J. Emerson, *New Journal of Physics* **16**, 013009 (2014).
- [60] E. H. Lieb and J. Yngvason, *Physics Reports* **310**, 1 (1999).
- [61] D. Janzing, P. Wocjan, R. Zeier, R. Geiss, and T. Beth, *Int. J. Theor. Phys.* **39**, 2717 (2000).
- [62] M. Horodecki *et al.*, *Phys. Rev. Lett.* **90**, 100402 (2003).
- [63] F. G. S. L. Brandão, M. Horodecki, J. Oppenheim, J. M. Renes, and R. W. Spekkens, *Physical Review Letters* **111**, 250404 (2013).
- [64] M. Horodecki and J. Oppenheim, *Nat. Commun.* **4**, 1 (2013).
- [65] G. Gour, M. P. Mller, V. Narasimhachar, R. W. Spekkens, and N. Y. Halpern, *Physics Reports* **583**, 1 (2015), The resource theory of informational nonequilibrium in thermodynamics.
- [66] N. Yunger Halpern, *Journal of Physics A: Mathematical and Theoretical* **51**, 094001 (2018).
- [67] V. Narasimhachar and G. Gour, *Nature Communications* **6**, 7689 (2015).
- [68] M. Lostaglio, D. Jennings, and T. Rudolph, *Nature Communications* **6**, 6383 (2015).
- [69] A. S. L. Malabarba, A. J. Short, and P. Kammerlander, *New Journal of Physics* **17**, 045027 (2015).
- [70] J. Åberg, *Phys. Rev. Lett.* **113**, 150402 (2014).
- [71] M. Lostaglio, K. Korzekwa, D. Jennings, and T. Rudolph, *Physical Review X* **5**, 021001 (2015).
- [72] M. Lostaglio, Á. M. Alhambra, and C. Perry, *Quantum* **2**, 52 (2018).
- [73] S. Bedkihal, J. Vaccaro, and S. Barnett, ArXiv e-prints (2016), 1603.00003.
- [74] P. Skrzypczyk, A. J. Short, and S. Popescu, arXiv:1302.2811 (2013).
- [75] P. Skrzypczyk, A. J. Short, and S. Popescu, *Nature Communications* **5**, 4185 (2014).
- [76] N. Yunger Halpern and J. M. Renes, *Phys. Rev. E* **93**, 022126 (2016).
- [77] L. Masanes and J. Oppenheim, ArXiv e-prints (2014), 1412.3828.
- [78] W. Pauli, *Handbuch der Physik* (Springer, Berlin, 1933), pp. 24 : 83–272.
- [79] W. Pauli, *Encyclopedia of Physics* (Springer, Berlin, 1958), p. 1 : 60.
- [80] R. P. Feynman, *Foundations of Physics* **16**, 507 (1986).
- [81] N. Margolus, *Annals of the New York Academy of Sciences* **480**, 487, <https://nyaspubs.onlinelibrary.wiley.com/doi/pdf/10.1111/j.1749-6632.1986.tb12451.x>.
- [82] M. F. Frenzel, D. Jennings, and T. Rudolph, *New Journal of Physics* **18**, 023037 (2016).
- [83] M. P. Woods, R. Silva, and J. Oppenheim, ArXiv e-prints (2016), 1607.04591.
- [84] P. Erker *et al.*, *Phys. Rev. X* **7**, 031022 (2017).
- [85] M. P. Woods, R. Silva, G. Pütz, S. Stupar, and R. Renner, ArXiv e-prints (2018), 1806.00491.
- [86] E. Ruch, *Theoretica Chimica Acta* **19**, 225 (1975).
- [87] E. Ruch, *Theoretica Chimica Acta* **38**, 167 (1975).
- [88] E. Ruch and B. Lesche, *J. Chem. Phys.* **69**, 393 (1978).
- [89] E. Ruch and A. Mead, *Theoretica Chimica Acta* **41**, 95 (1976).
- [90] E. Ruch, R. Schraner, and T. H. Seligman, *The Journal of Chemical Physics* **69**, 386 (1978).
- [91] D. Egloff, O. C. O. Dahlsten, R. Renner, and V. Vedral, *New Journal of Physics* **17**, 073001 (2015).
- [92] A. W. Marshall, I. Olkin, and B. C. Arnold, *Inequalities: theory of majorization and its applications* (Springer, 2010).
- [93] I. Marvian and R. W. Spekkens, *Phys. Rev. A* **90**, 062110 (2014).
- [94] P. Ao *et al.*, *Physical review letters* **62**, 3004 (1989).
- [95] K. Saito, M. Wubs, S. Kohler, Y. Kayanuma, and P. Hänggi, *Physical Review B* **75**, 214308 (2007).
- [96] L. Arceci, S. Barbarino, R. Fazio, and G. E. Santoro, *Physical Review B* **96**, 054301 (2017).
- [97] R. K. Malla, E. Mishchenko, and M. Raikh, *Physical Review B* **96**, 075419 (2017).
- [98] H. Kwon, H. Jeong, D. Jennings, B. Yadin, and M. S. Kim, *Phys. Rev. Lett.* **120**, 150602 (2018).
- [99] X. N. Feng and L. F. Wei, *Scientific Reports* **7**, 15492 (2017).
- [100] L. Del Rio, J. Åberg, R. Renner, O. Dahlsten, and V. Vedral, *Nature* **474**, 61 (2011).
- [101] J. Åberg, *Nat. Commun.* **4**, 1925 (2013).
- [102] J. M. Renes, *The European Physical Journal Plus* **129**, 153 (2014).
- [103] P. Faist, M. Berta, and F. Brandão, ArXiv e-prints (2018), 1807.05610.

- [104] R. Renner, *Security of Quantum Key Distribution*, PhD thesis, PhD Thesis, 2005, 2005.
- [105] N. Datta, IEEE T. Inform. Theory **55**, 2816 (2009).
- [106] M. Berta, *Quantum Side Information: Uncertainty Relations, Extractors, Channel Simulations*, PhD thesis, ETH Zürich, 2013.
- [107] F. Leditzky, *Relative entropies and their use in quantum information theory*, PhD thesis, U. of Cambridge, 2016.
- [108] M. M. Wilde, *Quantum Information Theory*, 2 ed. (Cambridge University Press, 2017).
- [109] C. E. Shannon, Bell Syst. Tech. J. **47**, 379 (1948).
- [110] P. Skrzypczyk, A. J. Short, and S. Popescu, Nature Communications **5**, 4185 (2014).
- [111] K. Korzekwa, M. Lostaglio, J. Oppenheim, and D. Jennings, New Journal of Physics **18**, 023045 (2016).
- [112] M. P. A. Fisher and L. Radzihovsky, Proceedings of the National Academy of Sciences **115**, E4551 (2018), <http://www.pnas.org/content/115/20/E4551.full.pdf>.
- [113] G. S. Engel *et al.*, Nature **446**, 782 (2007).
- [114] M. Sarovar, A. Ishizaki, G. R. Fleming, and K. B. Whaley, Nature Physics **6**, 462 EP (2010), Article.
- [115] H.-G. Duan *et al.*, Proceedings of the National Academy of Sciences **114**, 8493 (2017), <http://www.pnas.org/content/114/32/8493.full.pdf>.
- [116] H. C. H. Chan, O. E. Gamel, G. R. Fleming, and K. B. Whaley, Journal of Physics B: Atomic, Molecular and Optical Physics **51**, 054002 (2018).
- [117] A. E. Jaiilaubekov *et al.*, Nature Materials **12**, 66 EP (2012), Article.
- [118] G. M. Akselrod *et al.*, Nano Letters **14**, 3556 (2014).
- [119] R. H. Gilmore, E. M. Lee, M. C. Weidman, A. P. Willard, and W. A. Tisdale, Nano letters **17**, 893 (2017).
- [120] J. Lin *et al.*, Nature materials **17**, 261 (2018).
- [121] N. Yunger Halpern, *Toward Physical Realizations of Thermodynamic Resource Theories* (Springer International Publishing, Cham, 2017), pp. 135–166.
- [122] N. Lörch, C. Bruder, N. Brunner, and P. P. Hofer, Quantum Science and Technology **3**, 035014 (2018).
- [123] Z. Holmes, S. Weidt, D. Jennings, J. Anders, and F. Mintert, ArXiv e-prints (2018), 1806.11256.
- [124] Á. M. Alhambra, M. Lostaglio, and C. Perry, ArXiv e-prints (2018), 1807.07974.
- [125] A. Kitaev, D. Mayers, and J. Preskill, Phys. Rev. A **69**, 052326 (2004).
- [126] L. Mandel and E. Wolf, *Optical Coherence and Quantum Optics* (Cambridge UP, 1995).

Appendix: Resource-theory model for dissipative Landau-Zener problem

Let us sketch a resource-theory model for the dissipative LZ transition. Details are left for future work.

Clocks: The LZ problem involves a speed v and so involves time. In contrast, every thermal operation \mathcal{T} has time-translation covariance [71]: $e^{-iHt}\mathcal{T}(\rho)e^{iHt} = \mathcal{T}(e^{-iHt}\rho e^{iHt})$, if ρ denotes a state governed by the Hamiltonian H . We must therefore introduce a clock into our resource-theory formalism [50, 51, 53, 54, 69, 70, 82–85, 125]. In resource theories, clocks have been modeled as instances of more-general reference frames [69, 82–85]. A reference frame is a resource that effectively lifts a superselection rule such as energy conservation. A good clock reference frame occupies an even superposition over many energy eigenstates [50, 51, 53, 54, 70, 125] and so has substantial coherence. A clock can dictate which Hamiltonian governs the system of interest at any given instant.

The molecule’s clock: The molecular configuration φ serves as a clock in Eq. (2). The rotating chemical group, shown in Fig. 1, serves as the clock hand. When $\varphi = 0$, the hand effectively points to 12:00, and the *cis* Hamiltonian $H_{\text{elec}}(\varphi=0)$ governs the electronic DOF. When $\varphi = \pi$, the hand effectively points to 6:00, and the *trans* Hamiltonian $H_{\text{elec}}(\varphi=\pi)$ governs the electronic DOF.

A reliable clock hand has at least two properties: (i) Which number the hand points to can be distinguished. (ii) The clock hand sweeps across the clock face steadily. To serve as a good clock, therefore, the chemical group should have a well-defined angular position φ and a well-defined angular momentum ℓ_φ . The chemical group can have both due to its semiclassicality: Being large, the chemical group collides with other molecules frequently. The collisions localize the chemical group spatially. Being heavy, the chemical group is expected to have a large angular momentum: $\langle \ell_\varphi \rangle \sim \frac{\hbar}{mr}$, wherein m denotes the mode’s effective mass and r denotes the molecule’s radius. The configuration occupies a state analogous to a coherent state of light [82, 126] and to the Gaussian clock state in [83].

Evolution: As the molecule rotates, the clock hand ticks forward. To simplify the discussion, we will use the Schrödinger picture. In contrast, many thermodynamic-resource-theory calculations are performed in the interaction picture: Consider a system \mathcal{S} that interacts with a bath \mathcal{B} during a thermal operation \mathcal{T} . A Hamiltonian-conserving unitary U evolves $\mathcal{S}+\mathcal{B}$: $[U, H_{\mathcal{S}}+H_{\mathcal{B}}] = 0$. The conservation enables us to ignore the evolution generated by $H_{\mathcal{S}}+H_{\mathcal{B}}$.

We discretize $\varphi \in [0, 2\pi]$ into $2f$ values, for a fixed value of f :

$$H_{\text{mol}} = \sum_{j=0}^{2f-1} \left[H_{\text{elec}}(\varphi_j) \otimes |\varphi_j\rangle\langle\varphi_j| + \mathbb{1}_{\text{elec}} \otimes \frac{\ell_\varphi^2}{2m} \right]. \quad (31)$$

When $t = 0$, $\varphi_0 = 0$, and when $t = t_f$, $\varphi = \pi$. We extend the angle to be $\varphi \in [0, 2\pi)$, such that $\varphi_{2f} = \varphi_0$.

We model the evolution as a sequence of two alternating time steps: (i) A “tick operation” shifts the clock hand forward, changing the Hamiltonian $H_{\text{elec}}(\varphi)$ experienced by the electronic DOF. We model the electronic state as approximately constant during this time step. (ii) The new $H_{\text{elec}}(\varphi)$ evolves the electronic state for a time Δt . The greater the Δt , the more slowly the molecule rotates.

Speeds: This model has three regimes: the sudden-quench limit, the quantum-adiabatic limit, and intermediate speeds. Let us introduce these regimes in turn. To facilitate understanding, we temporarily suppose that the electronic DOF begins in an eigenstate $|\mathcal{E}_+(0)\rangle$ of $H_{\text{elec}}(0)$.

In the sudden-quench limit, $\Delta t \ll \frac{\hbar}{\varepsilon_+(\varphi)-\varepsilon_-(\varphi)}$ for all $\varphi \in [0, \pi]$. No intermediate $H_{\text{elec}}(\varphi)$ ’s have time to evolve the electronic DOF. The electronic state remains $|\mathcal{E}_+(0)\rangle$, while $H_{\text{elec}}(\varphi)$ changes drastically. The final electronic state may therefore have coherence relative to the final energy eigenbasis.

In the quantum-adiabatic limit, $\Delta t \gg \frac{\hbar}{\varepsilon_+(\varphi)-\varepsilon_-(\varphi)}$ for all φ . After the first time step, $H_{\text{elec}}(\varphi_1)$ evolves the electronic state $|\mathcal{E}_+(0)\rangle$. A matrix diagonal relative to the $H_{\text{elec}}(\varphi_0)$ eigenbasis represents the initial state, $|\mathcal{E}_+(0)\rangle\langle\mathcal{E}_+(0)|$, while an off-diagonal matrix represents $H_{\text{elec}}(\varphi_1)$. The off-diagonal elements change the state. The change is sizable, because Δt is large. In the $\Delta t \rightarrow \infty$ limit, the change evolves the state into an eigenstate of $H_{\text{elec}}(\varphi_1)$.

In the intermediate regime, $\Delta t \approx \frac{\hbar}{\varepsilon_+(\varphi)-\varepsilon_-(\varphi)}$. Each new $H_{\text{elec}}(\varphi)$ updates the state but not to an eigenstate of the instantaneous Hamiltonian.

Ticking operation: To introduce the ticking operation, we temporarily disregard the bath. The operator

$$U_{\text{tick}} := \mathbb{1}_{\text{elec}} \otimes \sum_{j=0}^{2f-1} |\varphi_{j+1}\rangle\langle\varphi_j| \quad (32)$$

rotates the molecule. The operator is unitary, $U_{\text{tick}}^\dagger U_{\text{tick}} = U_{\text{tick}} U_{\text{tick}}^\dagger = \mathbb{1}_{\text{elec}} \otimes \mathbb{1}_\varphi$, by the modularity of φ .

The system-and-clock Hamiltonian can generate U_{tick} if the clock evolves under a Hamiltonian proportional to its momentum [69, 78–81, 83]. This requirement stipulates, in our case, that $H_\varphi = c\ell_\varphi$. The constant $c \in \mathbb{R}$ can be set to one. This Hamiltonian has an eigenspectrum unbounded from below and so is unphysical. If the clock Hamiltonian were physical, we could use this result to model, resource-theoretically, a molecule tumbling by itself.

Nevertheless, we can use the ideal clock to understand how the molecule's angular DOF serves as an imperfect clock. The ideal clock's $H_\varphi \propto \ell_\varphi$ kicks the clock hand forward: H_φ generates a unitary $e^{-\frac{i}{\hbar}\ell_\varphi t}$ that evolves the clock as $|\varphi_j\rangle \mapsto e^{-\frac{i}{\hbar}\ell_\varphi t}|\varphi_j\rangle = |\varphi_j + t\rangle \equiv |\varphi_{j+1}\rangle$. Again, we have translated the notation of [69] into our notation.

Our clock's Hamiltonian equals the kinetic energy T in Eq. (2): $H_\varphi = \frac{(\ell_\varphi)^2}{2mr^2}$. This H_φ not only shifts the angular DOF forward, but also spreads out the DOF's state in position space. This spreading is not expected to change the state much, due to the chemical group's near-classicality. To reconcile the molecule's Hamiltonian with the quantum-clock formalism more precisely, one might adapt [83]. In [83], Woods *et al.* approximate the $H_c \propto \ell_\varphi$ clock with an oscillator whose Hilbert space has a finite dimensionality.

Dissipative ticking operation: Let us reincorporate the bath into the model. While rotating, the molecule jostles bath particles. They carry off energy dissipated as $H_{\text{elec}}(\varphi)$ changes.

To model the dissipation, we assume that the bath Hamiltonian's spectrum is dense and contains gaps of all sizes: For every electronic energy eigenstate $|\mathcal{E}_\pm(\varphi_j)\rangle$, $H_{\mathcal{B}}$ has eigenstates $|\mathcal{E}_j^\pm\rangle$ and $|\mathcal{E}_{j+1}^\pm\rangle$ such that the energy leaving the molecule enters the bath:

$$\langle \mathcal{E}_\pm(\varphi_j) | H_{\text{elec}}(\varphi_j) | \mathcal{E}_\pm(\varphi_j) \rangle + \langle \mathcal{E}_j^\pm | H_{\mathcal{B}} | \mathcal{E}_j^\pm \rangle = \langle \mathcal{E}_\pm(\varphi_j) | H_{\text{elec}}(\varphi_{j+1}) | \mathcal{E}_\pm(\varphi_j) \rangle + \langle \mathcal{E}_{j+1}^\pm | H_{\mathcal{B}} | \mathcal{E}_{j+1}^\pm \rangle. \quad (33)$$

For simplicity, we assume that \mathcal{B} has only one pair $|\mathcal{E}_j^\pm\rangle, |\mathcal{E}_{j+1}^\pm\rangle$ that satisfies condition (33), for each j . This assumption can be relaxed.

The isometry

$$\bar{U}_{\text{tick}} := \sum_{j=0}^{2f-1} \sum_{\mu=\pm} |\mathcal{E}_\mu(\varphi_j)\rangle \langle \mathcal{E}_\mu(\varphi_j)| \otimes |\varphi_{j+1}\rangle \langle \varphi_j| \otimes |\mathcal{E}_{j+1}^\mu\rangle \langle \mathcal{E}_j^\mu| \quad (34)$$

rotates the molecule while transferring energy from the molecule to the bath. \bar{U}_{tick} preserves the average energy by design: If ρ denotes the initial state of the molecule-and-bath composite, $\text{Tr}[\rho(H_{\text{mol}} + H_{\mathcal{B}})] = \text{Tr}[\bar{U}_{\text{tick}}\rho\bar{U}_{\text{tick}}^\dagger(H_{\text{mol}} + H_{\mathcal{B}})]$.

Three opportunities remain for future work: (i) \bar{U}_{tick} should be elevated from an isometry to a unitary. (ii) The energy conservation should be elevated from average to exact: \bar{U}_{tick} should commute with the global Hamiltonian. Exact conservation might require further use of reference frames. Some thermodynamic-resource-theory works, however, have required only average energy conservation [75]. (iii) The dissipation should be generalized to arbitrary molecule-bath coupling strengths. Suppose that the bath occupies the state $|\mathcal{E}_j^\pm\rangle$, being receptive to energy transfer. \bar{U}_{tick} transfers energy deterministically, reflecting strong coupling. But the coupling might be weak in physical reality. The molecule can have some probability < 1 of dissipating even if the bath is in $|\mathcal{E}_j^\pm\rangle$. One would adapt the first set-off equation in [72, App. B], attributed to [101], to many-level systems.

Sequence of time steps: Let ρ_{mol} denote the molecule's initial state. The first two time steps evolve the state as

$$\rho_{\text{mol}} \mapsto \text{Tr}_{\mathcal{B}} \left[\bar{U}_{\text{tick}} \left(\rho_{\text{mol}} \otimes \frac{e^{-\beta H_{\mathcal{B}}}}{Z_{\mathcal{B}}} \right) \bar{U}_{\text{tick}}^\dagger \right] =: \rho'_{\text{mol}} \quad (35)$$

$$\mapsto e^{-iH_{\text{mol}}\Delta t} (\rho'_{\text{mol}}) e^{iH_{\text{mol}}\Delta t}. \quad (36)$$

These two evolutions are repeated $f - 1$ times.